ADVANCED MATERIALS
www.advmat.de

Multimodal Tuning of Synaptic Plasticity Using Persistent Luminescent Memitters

Hongyu Bian, Xian Qin, Yiming Wu, Zhigao Yi, Sirui Liu, Yu Wang, Carlos D. S. Brites, Luís D. Carlos,* and Xiaogang Liu**

Mimicking memory processes, including encoding, storing, and retrieving information, is critical for neuromorphic computing and artificial intelligence. Synaptic behavior simulations through electronic, magnetic, or photonic devices based on metal oxides, 2D materials, molecular complex and phase change materials, represent important strategies for performing computational tasks with enhanced power efficiency. Here, a special class of memristive materials based on persistent luminescent memitters (termed as a portmanteau of "memory" and "emitter") with optical characteristics closely resembling those of biological synapses is reported. The memory process and synaptic plasticity can be successfully emulated using such memitters under precisely controlled excitation frequency, wavelength, pulse number, and power density. The experimental and theoretical data suggest that electron-coupled trap nucleation and propagation through clustering in persistent luminescent memitters can explain experience-dependent plasticity. The use of persistent luminescent memitters for multichannel image memorization that allows direct visualization of subtle changes in luminescence intensity and realization of short-term and long-term memory is also demonstrated. These findings may promote the discovery of new functional materials as artificial synapses and enhance the understanding of memory mechanisms.

1. Introduction

With an exponential increase in unstructured data connecting to the internet, computing speed and energy efficiency become challenging because of the speed-mismatch-induced memory wall between memory units and processors. Inspired by key features of human memory, researchers have devoted considerable effort to develop smart devices or machines that imitate social memory organization and information processing.[1–6] Indeed, memory behaviors with synaptic plasticity and neural computation have been demonstrated using electronic and magnetic devices comprising memristive materials, including inorganic semiconductors (e. g. TiO_2, MoO_2, MgO) and organic molecules.[7–18] Furthermore, optoelectronic memristors based on photosensitive mediums have also been realized through optical manipulation with enhanced resistive properties and recognition imaging contrast, closely resembling how light manipulation increases learning and memory through distinct retina–brain pathways and glutamate production.[19–25]

Compared with their electronic and magnetic counterparts, all-photonic memristors allow ultrafast operation speed, low power consumption, unlimited bandwidth, and precise spatiotemporal control, thus holding potential as ideal platforms for implementing on-chip, integrated photonic neuromorphic systems.[26–29] Currently, information encoding and decoding using all-photonic memristors are mainly achieved by varying transmittance under light irradiation through phase-change materials. Despite considerable efforts, synaptic plasticity modeling based on conventional all-photonic memory devices is generally limited to short-term plasticity and long-term plasticity. Particularly, experience-dependent plasticity or Ebbinghaus forgetting curve for memory consolidation has not been demonstrated. In this study, we demonstrate information encoding and decoding using a special class of persistent luminescence memitter (termed as a portmanteau of memory and emitter). We emulate different phases of postsynaptic responses by modulating the optical parameters of the memitter, including irradiation frequency, pulse number, power density, duration, and wavelength. Based on direct

Dr. H. Bian, Dr. X. Qin, Dr. Y. Wu, Dr. Z. Yi, S. Liu, Prof. X. Liu
Department of Chemistry
National University of Singapore
Singapore 117543, Singapore
E-mail: chmqinx@nus.edu.sg; chmlx@nus.edu.sg
Prof. Y. Wang, Prof. X. Liu
SZU-NUS Collaborative Center and International Collaborative Laboratory of 2D Materials for Optoelectronic Science and Technology of Ministry of Education
Institute of Microscale Optoelectronics
Shenzhen University
Shenzhen 518060, China
Prof. C. D. S. Brites, Prof. L. D. Carlos
Phantom-g
CICECO—Aveiro Institute of Materials
Department of Physics
Universidade de Aveiro
Aveiro 3810–193, Portugal
E-mail: lcarlos@ua.pt
Prof. X. Liu
Center for Functional Materials
National University of Singapore Suzhou Research Institute
Suzhou 215123, China
The ORCID identification number(s) for the author(s) of this article can be found under https://doi.org/10.1002/adma.202101895.

DOI: 10.1002/adma.202101895

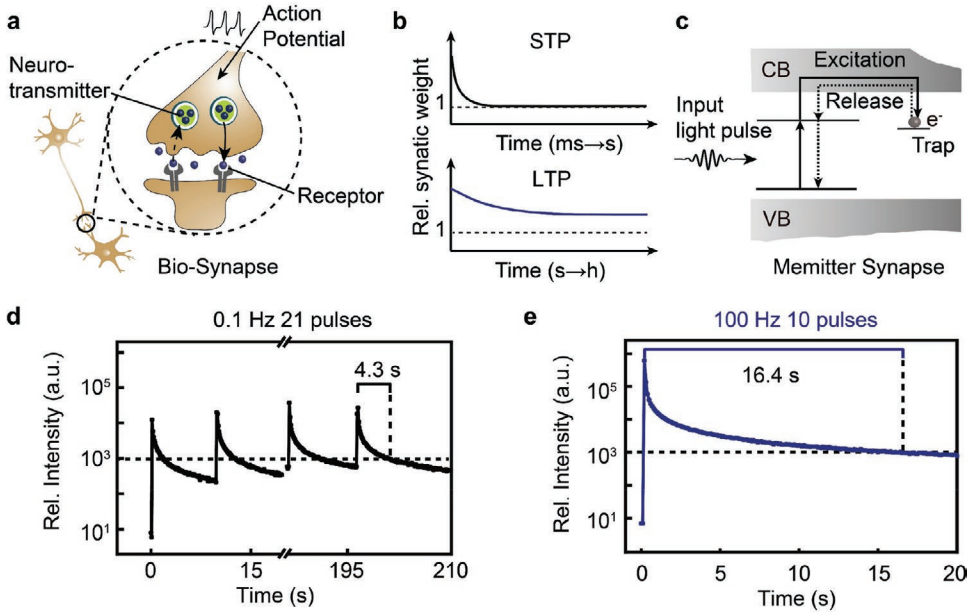

Figure 1. Bioinspired all-photonic synapse enabled by persistent luminescent memitters. a) Basic operation mechanism of a biosynapse synapse, in which electrical activity in the presynaptic neuron triggers the release of neurotransmitters that bind to receptors embedded in the plasma membrane of postsynaptic cells. b) STP and LTP are realized in a biosynapse under stimulation of different action potentials. c) Schematics showing the basic operation mechanism of a phosphor-based memitter synapse. d,e) Manipulation of persistent luminescence at varied pulse frequencies can be used to emulate LTP and STP. Artificial STP can be realized by subjecting the phosphor to a low pulse frequency (0.1 Hz) (d), while LTP is possible under a high pulse frequency of 100 Hz (e). The excitation and emission wavelengths are at 260 and 440 nm, respectively.

visualization of luminescence intensity changes, we also demonstrate multichannel image processing for short-term and long-term memory.

2. Result and Discussions

When an action potential reaches the presynaptic terminal, neurotransmitters are released from the neuron into the synaptic cleft with concomitant signal transmission. Frequent stimulation causes long-term enhancement in the strength of the synaptic connection (**Figure 1**a).[30] Short-term potentiation (STP) results from an increased probability of releasing neurotransmitters in response to presynaptic action potentials and lasts from milliseconds to several seconds. Meanwhile, long-term potentiation (LTP) is an increased synaptic response following an action potential and persists above the baseline response for hours or longer (Figure 1b).[31] We thus argued that it is possible to produce similar effects on synaptic plasticity by controlling the afterglow properties of PL phosphors through pulsed light stimulation (Figure 1c).[32–38] In principle, upon excitation, the electron of an emitting center is promoted to the excited state and then captured in defect-based traps, wherein the number of trapped electrons can be tuned by varying the excitation frequency. As demonstrated below, more trapped electrons induce higher-intensity and longer persistent luminescence under high-frequency excitation, which works as LTP. Meanwhile, it works as STP when there are fewer electrons in the traps under low-frequency excitation. During optical excitation and decay processes, electrons serve as neurotransmitters and defect-based traps are considered receptors, thereby enabling the synaptic plasticity of a biosynapse to be emulated in a luminescent memitters.

To validate this hypothesis, we prepared europium-doped calcium aluminate ($CaAl_2O_4$:0.5%Eu^{2+}) phosphors by a solid-state reaction and confirmed their crystallinity by X-ray powder diffraction and scanning electron microscopy (Figure S1, Supporting Information). Under 260 nm and 375 nm excitation, $CaAl_2O_4$:0.5%Eu^{2+} phosphors exhibited blue emission, corresponding to the $4f^65d^1 \rightarrow 4f^7$ transitions of Eu^{2+} (Figure S1, Supporting Information). The quantum yield of $CaAl_2O_4$:0.5%Eu^{2+} phosphors is 54.24% under 375 nm excitation. We then measured the luminescence decay curves of $CaAl_2O_4$:0.5%Eu^{2+} phosphors under 260 nm irradiation at various pulse frequencies. Under bursts of pulses at 0.1 Hz and repeated for 21 times, the persistent luminescence intensity increased to 10^4 with a dwell time of 4.3 s above the 10^3-threshold after stimulation (Figure 1d). Conversely, upon 10-pulse irradiation at 100 Hz (with an interval of 0.01 s), the luminescence intensity increased over a 10^5 with a dwell time of 16.4 s above the 10^3-threshold (Figure 1e). Based on these results, LTP is defined as any state in which the luminescence intensity is maintained above the 10^3-threshold for 10 s after pulsed stimulation, whereas STP is defined as any other state in which the luminescence intensity is below the 10^3-threshold at 10 s.

To further study the transformation from STP to LTP, $CaAl_2O_4$:0.5%Eu^{2+} phosphors were excited at 260 nm under different frequencies (0.1, 1, and 100 Hz) and numbers of pulses. The PL intensity at 10 s was maintained at over 10^3 under 1 Hz frequency irradiation with 10 pulses (**Figure 2**a), whereas that of 0.1 Hz irradiation decreased below 10^3 even after over 100 pulses. Furthermore, the afterglow intensity under 100 Hz

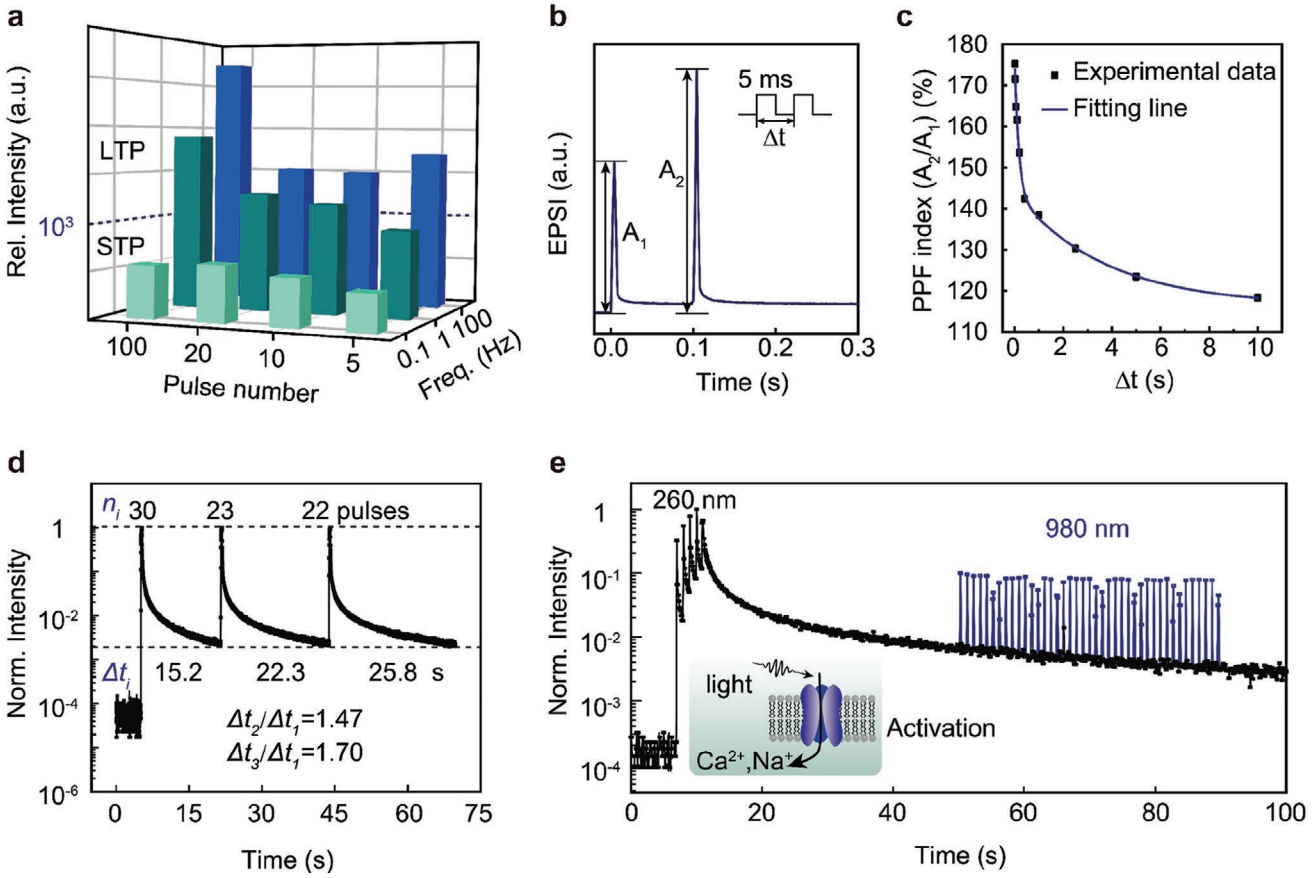

Figure 2. All-photonic synaptic plasticity and memory enabled by $CaAl_2O_4$:0.5%Eu^{2+} phosphors. a) Transformation from STP to LTP by controlling the luminescence intensity under irradiation of different pulse frequencies and numbers. The relative luminescence intensity was recorded 10 s after excitation. b) The EPSI triggered by a pair of presynaptic light pulses with a 0.1-s interval. A_1 and A_2 represent the amplitudes of the first and second EPSI, respectively. c) PPF index defined as A_2/A_1 plotted versus the pulse interval Δt. The fitting line indicates that the PPF index exponentially decreases with increasing Δt. Excitation and emission wavelengths are 375 and 444 nm, respectively. d) Experience-dependent plasticity realized under different excitation/emission cycles at 100 Hz. For cycle i ($i \geq 1$), the number of pulses needed to reach the set photoluminescence intensity is n_i and the time of the luminescence intensity decay to 0.2% is Δt_i. e) Memory recovery mimicked under 980 nm excitation. The normalized luminescence intensity at 440 nm upon 260 nm excitation was reactivated under pulsed 980 nm light stimulus (pulse width, 40 ms). Inserted is the schematic illustration of a typical ion channel in response to light simulation.

irradiation reached 10^3 after 5 pulses. Importantly, subsequent periodic irradiation resulted in a further increase in luminescence intensity, suggesting a transition from STP to LTP in artificial synapses.

In a biological synapse, paired-pulse facilitation (PPF) refers to a synaptic process where release of neurotransmitters can be activated by two proximal stimuli. A pair of light pulses (5-ms duration) with a time delay (Δt) of 100 ms was applied to the memitter (Figure 2b). The excitatory postsynaptic intensity (EPSI) triggered by the second pulse was larger than that of the first one. To evaluate the PPF of memitter-based artificial synapse, the PPF index was introduced and defined as PPF = $(A_2/A_1) \times 100\%$, where A_2 and A_1 represent the amplitude of EPSI for the second and the first pulse, respectively. The PPF index was plotted as a function of Δt (Figure 2c), with a maximum value of 175% (Δt = 100 ms). We recorded an exponential decay of the PPF index with increasing Δt. Such a decay reflects a learning pattern associated with frequently repeated training spikes in biological synapses.[39] EPSI responses to a train of 10 light pulses (5-ms duration) at 100 Hz (Figure S2, Supporting Information). The resulting EPSI was significantly improved compared with that induced by a single pulse, indicating that short-term learning and memory can be enabled by repeated presynaptic stimulations. The relation between EPSI and the pulse number showed a nonlinear response (Figure S2, Supporting Information). Furthermore, the EPSI gain, defined as A_{10}/A_1, was used to characterize the consolidation of post-synaptic response induced by a train of light pulses with different frequencies, where A_1 and A_{10} represent the peak values of EPSI of the first and the tenth pulse, respectively. The EPSI gain was plotted as a function of frequency in each spike train (Figure S2, Supporting Information). With an increase in the spike frequency increases, the EPSI gain enhanced from 1.4 (0.1 Hz) to 2.5 (100 Hz).

Extended retention of learned information is vital for memory. Ebbinghaus proposed that long-term memory can be achieved by repeating learned information after increasingly

large time gaps.[40] This experience-dependent effect is referred to metaplasticity, which is critical for attaining long-term memory (LTM).[41,42] To examine the suitability of the PL memitter for experience-dependent plasticity, we measured the persistent luminescence intensity through repeated irradiation (Figure 2d). We pumped photoluminescence intensity to a set level (normalized as 1) using 30 pulses and monitored the decay time required for afterglow intensity to reach 0.2%. In excitation cycle i ($i \geq 1$), the number of pulses needed is n_i and the time needed for afterglow intensity to reach 0.2% is Δt_i [s]. For $i = 1$, n_1 and Δt_1 were 30 and 15.2 s, respectively; for $i = 2$, n_2 and Δt_2 were 23 and 22.3 s, respectively; for $i = 3$, n_3 and Δt_3 were 22 and 25.8 s, respectively. In memory, the pumping and decay processes in persistent luminescence correspond to learning and forgetting, respectively. The decay time ratios of the second and third cycle to the first cycle at 0.2% intensity were 1.47 and 1.70, respectively. With persistent luminescence relaxing to the same state, the forgetting time gradually increased with i. Moreover, the required stimulus energy (pulse number) for memory recovery in the relearning episode ($i = 2, 3$) was considerably weaker than that in the first learning process ($i = 1$). Experience-dependent plasticity is obtained through repeated excitation in the persistent luminescent memitter. Similar phenomena were observed in chromium-doped zinc gallogermanate ($ZnGaGeO_4$:0.5%Cr^{3+}) and europium-doped strontium aluminate ($SrAl_2O_4$:1% Eu^{2+}) phosphors (Figures S3 and S4, Supporting Information). We have performed different experience-dependent plasticity plots under low-frequency (0.1 Hz) stimulation (Figure S5, Supporting Information). At 0.1-Hz excitation, the decay time ratios of the second and third cycle to the first cycle at 1% intensity were 1.12 and 1.15, respectively, whereas the decay time ratios increased to 1.18 and 1.27 at 1.7% intensity, respectively. This trend suggests that the decay time ratios between the second and third cycle to the first cycle at 0.2% intensity are likely to be much smaller than 1.12 and 1.15, respectively. The memitter-enabled metaplasticity was evidenced by increased synaptic weight with an increase in the stimulation cycle (Figures S6 and S7, Supporting Information).

Moreover, persistent luminescent memitters can emulate the behavior whereby some disappeared memory can be revitalized through optical stimulation.[43,44] To demonstrate the memory recall through light simulation, we applied a 980 nm laser to $CaAl_2O_4$:0.5%Eu^{2+} phosphors after 40 s luminescence decay and observed enhanced photoluminescence intensity (Figure 2e). This phenomenon was attributed to the 980 nm light moving electrons from the traps to the excited state as well as the radiative transition of Eu^{2+}.[45] Notably, the luminescence intensity was stronger upon wider pulse excitation because more photons were absorbed by the phosphors (Figures S8 and S9, Supporting Information).

To probe the mechanistic transformation from STP to LTP in all-photonic memory, we measured the thermoluminescence of $CaAl_2O_4$:0.5%Eu^{2+} phosphors under different pulse frequencies (**Figure 3**a). High frequencies resulted in high thermoluminescence intensities, which largely ascribed to the traps capturing more electrons. Using more pulses is an effective way to strengthen LTP, which is attributed to more generated electrons in traps, especially in deeper ones (Figure S10, Supporting Information). Notably, such excitation-associated dynamics has rarely been studied, and previously experimental and theoretical investigations were mainly focused on afterglow behavior under steady-state conditions.[46–48]

We reasoned that experience-dependent plasticity should originate from the diversity of electron trapping because the electrons are excited by different conditions. Further, we used density functional theory calculations to evaluate the vertical transition energy for the electron emission from the EuV_O center to Eu's 5d orbital or the conduction band minimum of the $CaAl_2O_4$ host (Supporting Information). Specifically, the energy required to release an electron from $2Eu^{3+}V_O$ state to $2Eu^{3+}V_O^{+1} + e_{CBM}$ state can be estimated from vertical absorption (Figure 3b). First, we consider re-excitation whereby one defect center ($2Eu^{3+}V_O$) as a seed is already in its excited state and another one ($2Eu^{2+}V_O$) at a different location is non-excited (Figure S11, Supporting Information). The calculated transition energy from the $2Eu^{2+}V_O$ to $2Eu^{3+}V_O + e_{CBM}$ state of the neighboring Eu^{2+} ion is 0.82 eV lower than that of the one at distance. In addition, both Bader charge analysis and charge density difference further confirmed that the excited electron in our simulation originates from the Eu's f electrons (Figure 3c). Next, we studied the release of an electron from an oxygen-vacancy-based trap. Calculated vertical transition energies from the $2Eu^{3+}V_O$ to $2Eu^{3+}V_O^{1+} + e_{CBM}$ state are 2.6 and 3.3 eV, respectively, with the two $2Eu^{3+}V_O$ traps are in close proximity or distant (Figure S11, Supporting Information). Considered together, a neighboring defect center can absorb excitation energy and release trapped electrons more easily than a distant one.

A mechanism, namely seed-centered electron-coupled trap clustering, is proposed based on quantum calculations and supported by experimentation. First, a seed is formed after a valence electron of Eu^{2+} is trapped within a defect. With increasing irradiation time, trap clusters form with captured electrons and grow in the center of the seed. Traps deepen because the Eu^{2+}'s electrons proximal to the seed are transferred to the defect more quickly than those farther away. Clusters stopped growing when the light was turned off, and trapped electrons near the seed release first because of shallow trap depths. Such phenomena are likely to occur because of the seed-induced lattice strain that facilitates electron redistribution within a short lattice distance. Thus, tuning of clusters by light in situ was realized, and traps can be tuned dynamically. This mechanism may be similar to that of memory formation and consolidation in neuroscience because a similar memory phenomenon is obtained from afterglow curves. Based on the clustering model, for experience-dependent plasticity, some electrons remain captured in traps far from the seed pairs after the first learning and forgetting. With the second excitation, the clusters grow and the traps deepen, resulting in a longer afterglow.

To further verify our clustering model, we tested the power-density-dependent properties of the luminescent memitter (Figure 3d and Figure S12, Supporting Information). Upon increasing the power density, the luminescence intensity decayed faster. Moreover, high intensity, short afterglow was observed at high excitation densities, while low intensity, long

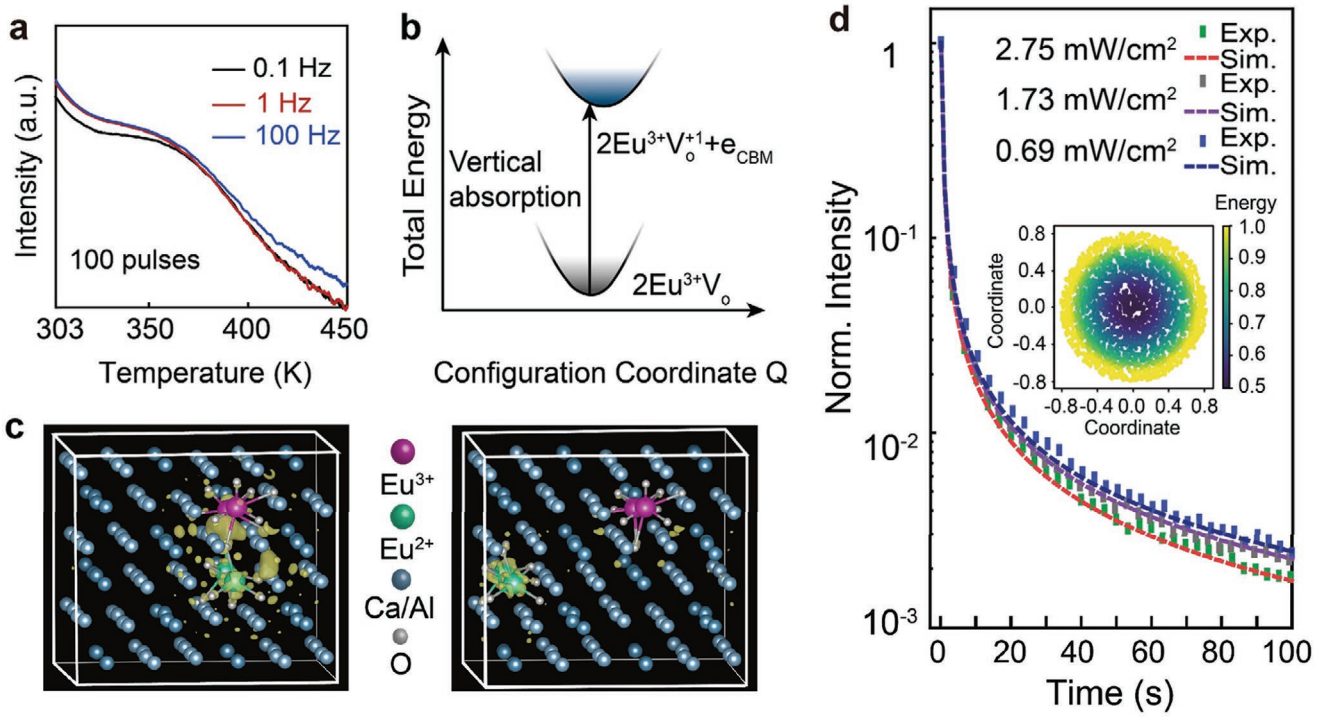

Figure 3. Proposed mechanism of all-photonic memory based on a persistent luminescent memitter. a) Thermoluminescence profiles of $CaAl_2O_4$:0.5% Eu^{2+} phosphors upon 100-pulse UV excitation (260 nm) at different frequencies (0.1, 1, and 100 Hz). b) 1D configuration coordinate diagram for release from oxygen vacancy-based trap to host conduction band minimum, which is related to the optical transition from $2Eu^{3+}V_O$ to $2Eu^{3+}V_O^{+1} + e_{CBM}$, where e_{CBM} denotes the electron released to the conduction band minimum of the host. c) Electron charge difference between $2Eu^{2+}V_O$ and $2Eu^{3+}V_O + e_{CBM}$ states when the emitter center is close to (left) or far from (right) the seed during re-excitation. The yellow isosurface represents the electron loss. d) Normalized and simulated luminescence curves of phosphors under excitation (λ_{ex} = 260 nm; λ_{em} = 440 nm) with different power densities (2.75, 1.73, and 0.69 mW cm^{-2} for 1, 1.6, and 4 s, respectively). Experimental data well match simulations with trap depths in the ranges of 0.425–0.625 eV, 0.425–0.825 eV, and 0.425–0.90 eV under low-, medium-, and high-power excitation, respectively. This suggests that the trap depth is inversely proportional to the pumping power. The light irradiation power is the same for every excitation process. Inset: Seed-centered defect clustering modeling of persistent luminescence memitters. The coordinate (0,0) denotes the position of the seed. Electrons are gradually trapped within non-seed defects that propagate from the seed toward its periphery. Simulations indicate that the defect depth increases with increasing spacing between the seed and the defect. The color bar represents the trap depth.

afterglow was observed at low excitation densities. In line with the seed-centered clustering model, higher power density induces smaller clusters because of the limited distance between different clusters. Thus, the traps do not deepen considerably, resulting in stronger and shorter afterglow. Meanwhile, the clusters are fewer and larger when the irradiation power density is lower, leading to longer and weaker persistent luminescence. We modeled seed-centered clustering under different excitation powers using Python (Figure S13, Supporting Information). To further verify the clustering model, we obtained luminescence decay curves under different excitation powers and cycles using Mathematica (Figure 3d and Figure S14, Supporting Information).

Based on the multi-store memory model, stimulus frequency distribution can affect sensory register, short-term memory (STM), and LTM.[49] For a proof of concept, we demonstrated image memory of letters **L** and **T** using a 5 × 5 array comprising memitters. The image memory was achieved by irradiating the array 100 times at frequencies of 100 and 1 Hz, respectively (**Figure 4**a). The relative intensity profiles (λ_{em} = 444 nm) of pixels E3 and A3 were recorded 1, 5, 10, and 20 s after the termination of laser excitation, respectively (Figure 4b,c, and Figure S15, Supporting Information). Importantly, owing to long-lasting persistent luminescence, the multi-store memory was achieved by directly comparing the patterns after different time intervals (1, 5, 10, 20 s). Letter **T** became invisible 20 s after exposure (100× excitation, 1 Hz), corresponding to STM. By comparison, letter **L** retained weak luminescence 20 s after exposure (100× excitation, 100 Hz), corresponding to LTM (Figure 4d).

3. Conclusion

We have achieved all-photonic memory on the basis of persistent luminescent memitters, enabling the emulation of STP, LTP, PPF, EPSI, STM, LTM, and experience-dependent plasticity. The high sensitivity synaptic response of memitters to frequency can be harnessed to manage information flows.[50,51] This study suggests that luminescence modulation of phosphors is a viable strategy for mimicking memory and programing neuromorphic computing. In addition, an electron trapped seed-centered clustering model was proposed to explain the change in persistent luminescence. This work may

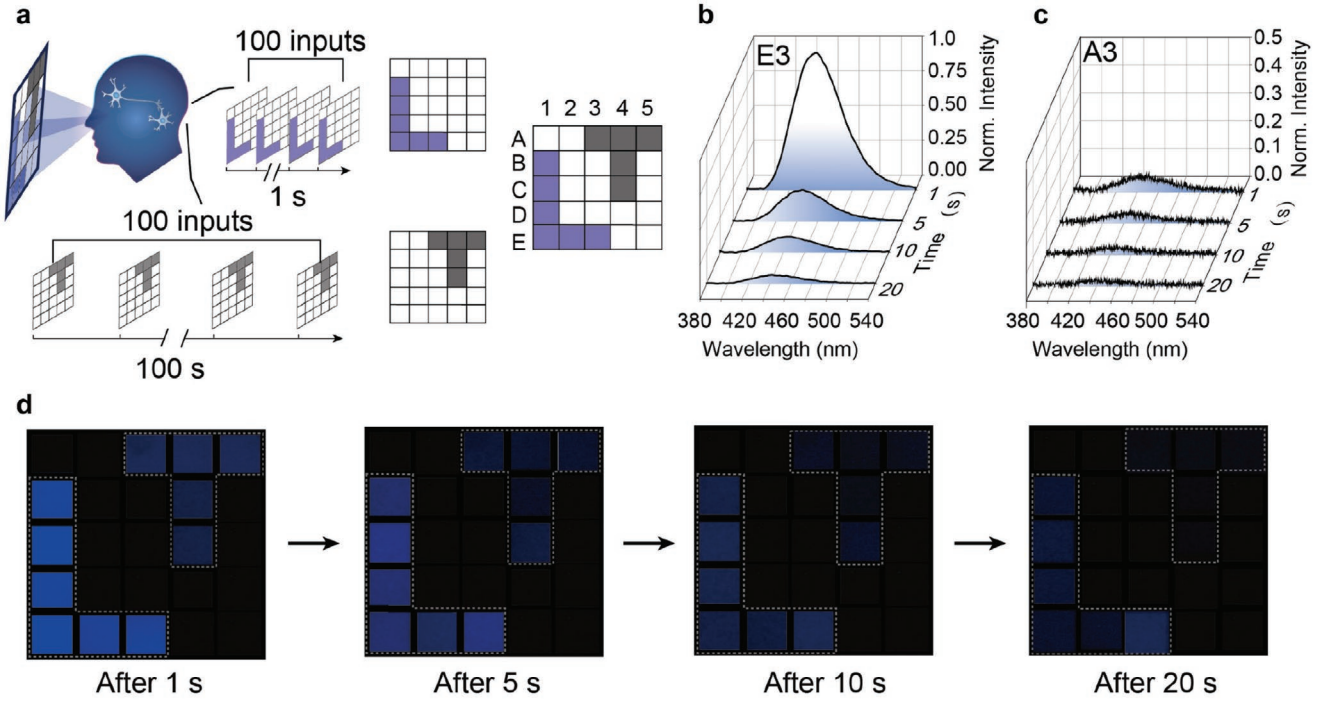

Figure 4. Image memory enabled by $CaAl_2O_4$:0.5% Eu^{2+} memitters. a) Design of multimodal memory in which a certain number of images are recorded, memorized, and consolidated in a 5 × 5 memitter array. In our design, graphic letters **L** and **T** were drawn through photoexcitation 100× at 100 and 1 Hz, respectively. b,c) Relative persistent luminescence intensity profiles (λ_{em} = 444 nm) of pixels E3 and A3, recorded at 1, 5, 10, and 20 s after cessation of irradiation. d) The corresponding blue-emitting pixels of letters **L** and **T**, recorded at different time intervals (1–20 s), reveal dual-modal capacity for LTM and STM.

provide insight into understanding memory mechanisms in bioscience, while potentially enabling low-power-consumption computing through luminescence.

4. Experimental Section

The experimental details are provided in the Supporting Information.

Supporting Information

Supporting Information is available from the Wiley Online Library or from the author.

Acknowledgements

The authors thank the Ministry of Education, Singapore (MOE2017-T2-2-110), Agency for Science, Technology, and Research (A*STAR) under its AME program (Grant No. A1883c0011 and A1983c0038), National Research Foundation, the Prime Minister's Office of Singapore under its NRF Investigatorship Programme (Award No. NRF-NRFI05-2019-0003), the King Abdullah University of Science and Technology (KAUST) Office of Sponsored Research (OSR) under Award No. OSR-2018-CRG7-3736, and the National Natural Science Foundation of China (21771135, 21871071). C.D.S.B. and L.C. acknowledge the project CICECO-Aveiro Institute of Materials, UIDB/50011/2020 and UIDP/50011/2020, financed by Portuguese funds through the FCT/MEC and when appropriate co-financed by FEDER under the PT2020 Partnership Agreement. The authors acknowledge Professor X. Chen and Dr. M. A. Hernández-Rodríguez for helpful discussion.

Conflict of Interest

The authors declare no conflict of interest.

Data Availability Statement

The data that support the findings of this study are available from the corresponding author upon reasonable request.

Keywords

image memorization, persistent luminescence, photonic memory, synaptic plasticity

Received: March 9, 2021
Revised: April 2, 2021
Published online:

[1] K. Roy, A. Jaiswal, P. Panda, *Nature* **2019**, *575*, 607.
[2] Z. Wang, H. Wu, G. W. Burr, C. S. Hwang, K. L. Wang, Q. Xia, J. J. Yang, *Nat. Rev. Mater.* **2020**, *5*, 173.
[3] V. K. Sangwan, M. C. Hersam, *Nat. Nanotechnol.* **2020**, *15*, 517.
[4] S. T. Keene, C. Lubrano, S. Kazemzadeh, A. Melianas, Y. Tuchman, G. Polino, P. Scognamiglio, L. Cinà, A. Salleo, Y. van de Burgt, F. Santoro, *Nat. Mater.* **2020**, *19*, 969.
[5] M. M. Shulaker, G. Hills, R. S. Park, R. T. Howe, K. Saraswat, H.-S. P. Wong, S. Mitra, *Nature* **2017**, *547*, 74.
[6] M. A. Zidan, J. P. Strachan, W. D. Lu, *Nat. Electron.* **2018**, *1*, 22.

[7] T. Li, F. Hong, K. Yang, B. Yue, N. Tamura, H. Wu, Z. Cheng, C. Wang, *Sci. Bull.* **2020**, *65*, 631.
[8] D. B. Strukov, G. S. Snider, D. R. Stewart, R. S. Williams, *Nature* **2008**, *453*, 80.
[9] L. Liu, C. Zhou, X. Shu, C. Li, T. Zhao, W. Lin, J. Deng, Q. Xie, S. Chen, J. Zhou, R. Guo, H. Wang, J. Yu, S. Shi, P. Yang, S. Pennycook, A. Manchon, J. Chen, *Nat. Nanotechnol.* **2021**, *16*, 277.
[10] S. Choi, J. Yang, G. Wang, *Adv. Mater.* **2020**, *32*, 2004659.
[11] C. Liu, H. Chen, S. Wang, Q. Liu, Y. G. Jiang, D. W. Zhang, M. Liu, P. Zhou, *Nat. Nanotechnol.* **2020**, *15*, 545.
[12] A. A. Bessonov, M. N. Kirikova, D. I. Petukhov, M. Allen, T. Ryhänen, M. J. A. Bailey, *Nat. Mater.* **2015**, *14*, 199.
[13] T. Ohno, T. Hasegawa, T. Tsuruoka, K. Terabe, J. K. Gimzewski, M. Aono, *Nat. Mater.* **2011**, *10*, 591.
[14] V. K. Sangwan, H. S. Lee, H. Bergeron, I. Balla, M. E. Beck, K. S. Chen, M. C. Hersam, *Nature* **2018**, *554*, 500.
[15] Y. Van De Burgt, E. Lubberman, E. J. Fuller, S. T. Keene, G. C. Faria, S. Agarwal, M. J. Marinella, A. Alec Talin, A. Salleo, *Nat. Mater.* **2017**, *16*, 414.
[16] C. Liu, X. Yan, X. Song, S. Ding, D. W. Zhang, P. Zhou, *Nat. Nanotechnol.* **2018**, *13*, 404.
[17] K. Yue, Y. Liu, R. K. Lake, A. C. Parker, *Sci. Adv.* **2019**, *5*, eaau8170.
[18] R. Yang, H. M. Huang, Q. H. Hong, X. B. Yin, Z. H. Tan, T. Shi, Y. X. Zhou, X. S. Miao, X. P. Wang, S. B. Mi, C. L. Jia, X. Guo, *Adv. Funct. Mater.* **2018**, *28*, 1704455.
[19] J. Y. Mao, L. Zhou, X. Zhu, Y. Zhou, S. T. Han, *Adv. Opt. Mater.* **2019**, *7*, 1900766.
[20] F. Zhou, Z. Zhou, J. Chen, T. H. Choy, J. Wang, N. Zhang, Z. Lin, S. Yu, J. Kang, H. S. P. Wong, Y. Chai, *Nat. Nanotechnol.* **2019**, *14*, 776.
[21] D. C. Fernandez, P. M. Fogerson, L. Lazzerini Ospri, M. B. Thomsen, R. M. Layne, D. Severin, J. Zhan, J. H. Singer, A. Kirkwood, H. Zhao, D. M. Berson, S. Hattar, *Cell* **2018**, *175*, 71.
[22] H. Zhu, N. Wang, L. Yao, Q. Chen, R. Zhang, J. Qian, Y. Hou, W. Guo, S. Fan, *Cell* **2018**, *173*, 1716.
[23] X. Guan, Y. Wang, C. H. Lin, L. Hu, S. Ge, T. Wan, A. Younis, F. Li, Y. Cui, D. C. Qi, D. Chu, X. D. Chen, T. Wu, *Appl. Phys. Rev.* **2020**, *7*, 031401.
[24] H. L. Park, H. Kim, D. Lim, H. Zhou, Y. H. Kim, Y. Lee, S. Park, T. W. Lee, *Adv. Mater.* **2020**, *32*, 1906899.
[25] S. Zhou, B. Peng, *J. Semicond.* **2020**, *41*, 072906.
[26] W. Zhang, R. Mazzarello, M. Wuttig, E. Ma, *Nat. Rev. Mater.* **2019**, *4*, 150.
[27] Z. Cheng, C. Ríos, W. H. P. Pernice, C. David Wright, H. Bhaskaran, *Sci. Adv.* **2017**, *3*, e1700160.
[28] C. Rios, M. Stegmaier, P. Hosseini, D. Wang, T. Scherer, C. D. Wright, H. Bhaskaran, W. H. P. Pernice, *Nat. Photonics* **2015**, *9*, 725.
[29] J. Feldmann, N. Youngblood, C. D. Wright, H. Bhaskaran, W. H. P. Pernice, *Nature* **2019**, *569*, 208.
[30] A. Vaiserman, O. Lushchak in *Neuroscience*, 3rd ed. (Eds: D. Purves, G. J. Augustine, D. Fitzpatrick, W. C. Hall, A.-S. Lamantia, J. O. Mcnamara, S. M. William), Sinauer Associates, Inc., Sunderland, MA, USA **2019**.
[31] W. B. Matthews, *Br. Med. J.* **1976**, *2*, 1202.
[32] Z. Pan, Y.-Y. Lu, F. Liu, *Nat. Mater.* **2012**, *11*, 58.
[33] Y. Li, M. Gecevicius, J. Qiu, *Chem. Soc. Rev.* **2016**, *45*, 2090.
[34] J. Xu, S. Tanabe, *J. Lumin.* **2019**, *205*, 581.
[35] Y. M. Yang, Z. Y. Li, J. Y. Zhang, Y. Lu, S. Q. Guo, Q. Zhao, X. Wang, Z. J. Yong, H. Li, J. P. Ma, Y. Kuroiwa, C. Moriyoshi, L. L. Hu, L. Y. Zhang, L. R. Zheng, H. T. Sun, *Light: Sci. Appl.* **2018**, *7*, 88.
[36] A. N. C. Neto, O. L. Malta, *Nature* **2021**, *590*, 396.
[37] D. Kulesza, P. Bolek, A. J. J. Bos, E. Zych, *Coord. Chem. Rev.* **2016**, *325*, 29.
[38] J. Yang, Y. Liu, D. Yan, H. Zhu, C. Liu, C. Xu, L. Ma, X. Wang, *Dalton Trans.* **2016**, *45*, 1364.
[39] P. Gkoupidenis, D. A. Koutsouras, G. G. Malliaras, *Nat. Commun.* **2017**, *8*, 15448.
[40] H. Ebbinghaus, *Ann. Neurosci.* **2013**, *20*, 155.
[41] W. C. Abraham, *Nat. Rev. Neurosci.* **2008**, *9*, 387.
[42] W. C. Abraham, M. F. Bear, *Trends Neurosci.* **1996**, *19*, 126.
[43] P. Rajasethupathy, S. Sankaran, J. H. Marshel, C. K. Kim, E. Ferenczi, S. Y. Lee, A. Berndt, C. Ramakrishnan, A. Jaffe, M. Lo, *Nature* **2015**, *526*, 653.
[44] X. Liu, S. Ramirez, P. T. Pang, C. B. Puryear, A. Govindarajan, K. Deisseroth, S. Tonegawa, *Nature* **2012**, *484*, 381.
[45] Y. Zhuang, L. Wang, Y. Lv, T. L. Zhou, R. J. Xie, *Adv. Funct. Mater.* **2018**, *28*, 1705769.
[46] J. J. Joos, K. Korthout, L. Amidani, P. Glatzel, D. Poelman, P. F. Smet, *Phys. Rev. Lett.* **2020**, *125*, 33001.
[47] J. Hölsä, T. Laamanen, M. Lastusaari, M. Malkamäki, J. Niittykoski, P. Novák, *Radiat. Phys. Chem.* **2009**, *78*, S11.
[48] X. Ou, X. Qin, B. Huang, J. Zan, Q. Wu, Z. Hong, L. Xie, *Nature* **2021**, *590*, 410.
[49] B. H. Ross, I. Boot, S. van Dantzig, *The Psychology of Learning and Motivation : Advances in Research and Theory*, Vol. *54*, Academic Press, Cambridge, MA, USA **2011**.
[50] H. Liu, M. Wei, Y. Chen, *Nanotechnol. Rev.* **2018**, *7*, 443.
[51] L. F. Abbott, W. G. Regehr, *Nature* **2004**, *431*, 796.